Multiscale Approach for Dehazing Using the STRESS Framework

Vincent Jacob Whannou de Dravo and Jon Yngve Hardeberg▲

The Norwegian Colour and Visual Computing Laboratory, Faculty of Computer Science and Media Technology,
Gjøvik University College, N-2802 Gjøvik, Norway
E-mail: vincent.whannou.de.dravo@gmail.com

Abstract. *Models that researchers often use for the dehazing task are based on the Koschmieder law. In this article, we use the STRESS (Spatio-Temporal Retinex-inspired Envelope with Stochastic Sampling) model for the dehazing task. In our work, we demonstrate theoretically and empirically how the parameters in the STRESS framework can be set for dehazing. We then propose a new algorithm for haze removal, based on the model of the (STRESS) framework, which combines edge detection and Hidden Markov Model (HMM) to solve the problem. Experiments show that our approach yields more visibility—based on some metrics and psychophysical tests—than most of the state-of-the-art approaches.* ⓒ *2016 Society for Imaging Science and Technology.*
[DOI: 10.2352/J.ImagingSci.Technol.2016.60.1.010409]

INTRODUCTION

Outdoor applications of visual media such as broadcasting winter sport events, video surveillance, and driver assistance systems[1] are frequently shot in adverse weather conditions in the presence of atmospheric particles[2] which cause fog or haze. On the other hand, fog or haze is very useful in the artistic domain[3-5] through simulation or painting for instance. In the Renaissance, the painter Leonardo da Vinci, in his book *Treatise on Painting*, employed for the first time, the term aerial perspective—also known as atmospheric perspective. Narasimhan and Nayar,[6] define this painting technique in the following terms: Colors become weaker in proportion to their distance from the person who is looking at them. Here, in this work, we propose an algorithm which will allow us to get more visibility for an image taken in hazy or foggy conditions. Phenomena such as haze, fog, dust, mist, and cloud are technically classified as aerosol, a colloid of fine solid particles or liquid droplets in air or another gas which can be natural or not.[7] Fog and forest mist, for instance, are classified as natural phenomena whereas haze, dust, or smoke are classified as artificial ones. These phenomena differ mainly in the types and the sizes of the particles involved and their concentration in space.[2] According to Ref. 9, a theory that explains haze or fog phenomena well, the Mie scattering theory or the Lorenz–Mie theory,[10] derived from the Maxwell's equation. The Mie scattering model, by allowing an explanation of the white color of cloud, differs from the Rayleigh theory which allows the explanation of the blue color of the sky. McCartney[8] explains that the Rayleigh scattering model breaks down when particle size becomes larger than around 10% of the wavelength of the incident radiation. At that point, the Mie scattering model approximates the phenomenon better.[9] Due to the high number of parameters to be considered, Simonot and his colleagues[11] divide the main scattering model roughly into two main categories: (1) single scattering and (2) multiple scattering. Single scattering refers to a particle which scatters the light once.

In this article, we propose to use the STRESS framework[13]—we show in a previous article[54] that STRESS, considered as an image enhancement algorithm, could be seen as a good heuristics for the dehazing task.

In the next section, we will present some relevant articles related to our procedure, followed by the theoretical part and the method that we propose. The section *Experiment and Results* will describe our experiment setup and finally, we will conclude and give an idea of what could be the future work.

STATE OF THE ART

Dehazing algorithms are often divided into two main groups. The first group could be those algorithms which based their analysis more on an image processing approach than a physics one and the second group could be the ones which worked directly with the physical model. That is precisely the reason why we can now argue that there exist three major types of dehazing algorithms:

- The first group belongs to the image enhancement group algorithms, where dehazing is done by using image enhancement techniques such as histogram equalization, homomorphic filter, wavelet transform, Retinex algorithms, ACE,[12] STRESS,[13] luminance, and contrast enhancement.

- The second group of algorithms for dehazing purpose takes mainly into account a degradation model to remove haze from hazy images. Most of the algorithms in this group, considered as a state of the art for dehazing, used this approach due to the fact that they take into consideration the haze physical model to restore the haze-free image. There are two main

approaches used for this second method of dehazing. The first approach is the stereo or the multi-views approach where the depth of the haze or other types of data are estimated by using two or more images.[2,6,15] The other one uses a single image.

- The third group is the one which uses a combination of both the first group and the second group. The work of Refs. 14, 16 illustrates perfectly this algorithm process.

In this part, we will begin our review with the first group, followed by the third group, and the second group will be presented at the end.

From the first group, people are often using histogram equalization and other image enhancement algorithms such as Retinex and ACE. Most of the time, these algorithms are combined with insight from the second category. One main characteristic of the first group is that they are physiological/heuristical basis and often point operator or point process; some of them can use neighborhood operator as well. For those which are based on point process, some information or statistics can be collected globally and for others, local information is taken into account as for the case of Land/McCann's Retinex algorithm.

For the third type, some authors[17] proposed to use mainly an image enhancement based approach, by combining an adaptive Single Scale Retinex (SSR) with the Dark Channel Prior (DCP), developed by Ref. 18. The idea consists of the establishment of a relationship between the depth and the Retinex scale factor: a small scale gauss filter is well suited for far objects whereas for near objects, we have the inverse procedure.[19] To take their decision, they have estimated beforehand the transmission in the same way as in Ref. 18. The second algorithm related to the third group is developed in Ref. 16. Here also the Retinex is used. Authors in Ref. 19 designed an algorithm where the physical model of haze is mixed with a Retinex and an adaptive filter approach. The algorithm works in three steps. The first one consists of the estimation of the airlight by selecting, as in Ref. 18, the 0.1% of brightest pixels in the dark channel. The second employs a Retinex method to extract the antibrightness image of HIS (Hue–Saturation–Intensity) color space. The third step involves the estimation of the transmission thanks to the computation of the antibrightness. After all this, the recovered scene is estimated. In Ref. 14 the authors used the YC_bC_r—Y for luminance and two chrominance components C_b and C_r, representing the blue- and red-difference chroma components, respectively—instead of HIS as previously. In this work, the authors assessed the transmission by using a multiscale Retinex, and the airlight, by following a procedure as defined in Ref. 18. The last algorithm of the third group that we present, is the work of Galdran and colleagues, as described in Ref. 20. In this algorithm based on ACE, the airlight and the transmission are loosely estimated, respectively by taking the maximum intensity for each channel—almost the same procedure is adopted in Ref. 18—and by 1/2. The dehazing task is then switched into an optimization problem and the haze-free image is restored.

For the remainder of this section, some of the second type of algorithms will be presented. In the work of Fattal, as we can see in Ref. 21, the assumption is that the shading and the transmission function are locally statistically incorrelated. The dehazing issue is solved by estimating mainly the transmission twice and by finding a good approximation of this parameter in iterative fashion. The airlight is roughly estimated first and refined later, and finally, the haze-free solution is deduced from these computations.

In his work in Ref. 23, Tan made two assumptions to master the haze physical model: the haze-free image has more contrast than the hazy image and the airlight tends to be smooth. From this perspective, the airlight parameter is the main parameter estimated. The others are then deduced from that point. Reference 18 introduces the Dark Channel Prior (DCP or DC) concept. The prior is stated as follows: In most of the non-sky patches considering a haze-free image, at least one color channel has some pixels whose intensities are very low and close to zero. From this definition, the transmission and the airlight are estimated. Finally, the haze-free image is computed. The work in Ref. 24, is built on a series of assumptions making authors infer the atmospheric veil and have a first restoration. They then refined the solution by applying corner smoothing and tone mapping. In his articles,[25–27] Gibson and his co-authors use the (DCP) that they customized, by slightly adding new hypothesis. Finally in Ref. 28, the main authors of previous articles use a locally adaptive Wiener filter to speed up the fog removal process.

Other interesting works, about dehazing using a physical model, are within Refs. 2, 34–37. In the next section, we will present the STRESS framework and show how we could use it for the dehazing task.

MODEL ANALYSIS AND MODEL DEVELOPMENT

In this section, we will present the STRESS framework. We will see that the introduction in the STRESS framework of the concept of minimum envelope will allow us to solve the problem on near objects of the scene. Later on, we will combine this characteristic, in addition to Hidden Markov Model (HMM) and edge detection to solve a more general problem. There are two variants of Koschmieder haze physical law used in the literature. The first is as follows:

$$I(x) = J(x)t(x) + (1 - t(x))A(x), \qquad (1)$$

where I is the observed image, J is the scene radiance, A the global atmospheric light, and t the medium transmission. Here too, there are many approaches to solve this haze model. The goal here is to remove the fog by estimating, J, A, and t. This first expression can be found in Refs. 18, 21.

The second widely used formula or its variant is presented in Ref. 6 and a variant in Refs. 23 or 24:

$$E = I_\infty \rho e^{-\beta d} + (1 - e^{-\beta d})I_\infty, \qquad (2)$$

where I_∞ represents the sky intensity and the term $e^{-\beta d}$ represents the transmission with β being the scattering coefficient of the atmosphere; it represents the ability of a unit

J. Imaging Sci. Technol.
IS&T International Symposium on Electronic Imaging 2016
Color Imaging XXI: Displaying, Processing, Hardcopy, and Applications

010409-2

Jan.-Feb. 2016

COLOR-353.2

Figure 1. From left to right Original image (a), result with DCP in middle (b) and STRESS with parameter $n_i = 150$ and $n_s = 5$ (c). Image taken in Gjøvik—Lake Mjøsa—at the beginning of the winter 2014–2015. As we can see, the fog on near objects is well removed, far objects still have fog and we do not obtain any saturation effect with (c), that we have in the case of (b).

volume of atmosphere to scatter light in all directions and d, the depth of the scene point from the observer.

STRESS

The STRESS framework[13]—Spatio-temporal Retinex-inspired Envelope with Stochastic Sampling—has many applications.[13,37,38] In this part, we will deal with constructing the enhancement of a hazy image and by doing this, we are going to elaborate on the stretching part of the framework. The STRESS algorithm is derived from two previous works.[39,40] As in Ref. 39, the envelope concept is used but instead of using just the maximum envelope, the authors also designed the minimum envelope. As we will see in the following lines, the minimum envelope approximates the haze physical model well for some scenarios. From Ref. 40, the random spray technique is mimicked. The spray is a circular patch centered at the current pixel p_0, in which the samples p_i ($\neq p_0$) are taken in order to reconstruct the initial signal. For a given iteration, all the samples are different from each other. The framework uses a locality and globality principle. Let us take a look at the formal definition of the two envelopes $E^{\min}$ and $E^{\max}$:

$$s_i^{\max} = \max_{j \in \{0...M\}} p_j; \qquad s_i^{\min} = \min_{j \in \{0...M\}} p_j$$

$$r_i = s_i^{\max} - s_i^{\min}; \qquad v_i = \begin{cases} 1/2 & \text{if } r_i = 0, \\ (p_0 - s_i^{\min})/r_i & \text{else} \end{cases}$$

$$\bar{r} = \frac{1}{N} \sum_{i=1}^{N} r_i; \qquad \bar{v} = \frac{1}{N} \sum_{i=1}^{N} v_i$$

$$E^{\min} = p_0 - \bar{v}\bar{r}; \qquad E^{\max} = p_0 + (1 - \bar{v})\bar{r} = E^{\min} + \bar{r}$$

$$(3)$$

where,

- p_j is a pixel taken in the spray and different from p_0 (the current pixel) with j being the current sample;
- i the current iteration and N (or n_i) the total number of Iterations;
- M (or n_s) the number of samples for a given iteration i;
- v_i the relative value of the center and the averaging ranges r_i;

- $E^{\min}$ (resp. $E^{\max}$) the minimum envelope (resp. the maximum envelope).

New Model

The first experiment that we did on this project is related to the comparison between some spatial color algorithms as in Refs. 41, 42 and some of state-of-the-art algorithms.[18,24] More than 200 images were processed. This first experiment visually shows that STRESS removes the haze at least for near objects and ACE[12,42]—as well as STRESS—gives a nonsaturated effect on dense haze. An example is given in Figure 1. The other point is that some dehazing articles have already used ACE, but not STRESS.

Now the question is: If STRESS is able to remove fog on near objects or from a dense fog without getting saturation effects in the sky as in the case of DCP, perhaps we could use it to dehaze any kind of haze. So the question which comes to our mind reads: if STRESS can remove fog from any kind of fog then surely it can remove fog from a homogeneous haze—even if in real world, a homogeneous haze is extremely rare; we are making this hypothesis for abstraction manipulation and because STRESS processes each pixel the same way. We choose 10 natural images—images which do not contain haze—on the internet and apply a thin layer on them with a different density to simulate the (dense) homogeneous haze on them. The experiment shows that the haze is well removed, as you can see in Figure 2. The idea originates from these previous experiments which show that there might be a link between the STRESS model and the haze physical model. To check this hypothesis, we will check the STRESS output with the envelope values, which is expressed by:

$$P_{\text{STRESS}} = \frac{P_0 - E^{\min}}{E^{\max} - E^{\min}}. \qquad (4)$$

In the work[23] as shown in Eq. (2), the haze model is a bit different from Eq. (1). According to the formula in Eq. (2) above and by changing some variables, we can rewrite the model as follows:

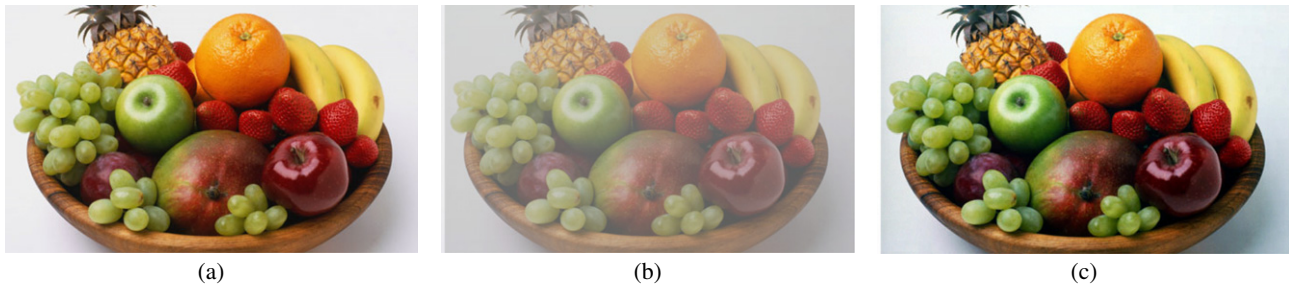$$I(x) = J(x)t_1(x) + (1 - t_2(x))A(x). \qquad (5)$$

(a)   (b)   (c)

Figure 2. The original image (right), the synthesized homogeneous fog (middle), the haze-free using STRESS with $n_i = 100$ and $n_s = 15$ (right). For this experiment, with homogeneous fog, we noticed that by taking more samples, the output of STRESS more closely resembles the original image. Original taken from www.theguardian.com

Observation 1. *The minimum envelope $E^{\min}$ in the STRESS framework is a solution of the haze physical model defined in Eq. (5).*

The multiplicative factor t on the right-hand side in Eq. (1) is replaced in the above formula by t_1 and t_2. So now let us consider the model expressed by Eq. (5). By considering the two definitions of the envelopes $E^{\min}$ and $E^{\max}$, we can write:

$$p_0 = E^{\max} - (1 - \bar{v})\bar{r} \qquad (6)$$
$$p_0 = E^{\min} + \bar{r} - (1 - \bar{v})\bar{r}$$
$$p_0 = E^{\min} + [1 - (1 - \bar{v})]\bar{r}. \qquad (7)$$

From Eq. (7), we can find $\bar{w} \in [0, 1]$ such that $\bar{w} = 1 - \bar{v}$. Since we know that $\bar{v}$ or $\bar{r}$ are elements of $[0, 1]$ from Ref. 48, we can then write Eq. (7) as the following:

$$p_0 = E^{\min} + (1 - \bar{w})\bar{r}. \qquad (8)$$

Let us pose now $\bar{w}_1 = 1$ and $\bar{w}_2 = \bar{w}$. So the above relationship can then be written:

$$p_0 = E^{\min}\bar{w}_1 + (1 - \bar{w}_2)\bar{r}. \qquad (9)$$

In our case, $E^{\min}$ concords with the radiance J and p_0 to the input pixel value. We can therefore see the link between Eq. (9) above and Eq. (5). Also from Ref. 18, it is said that the transmission $t \approx 0$ for a distant object. And from Ref. 22, we know that a good estimation of the transmission parameter should be such that $t \in [0, 1]$, which obviously is the case for our two pseudo-transmissions $\bar{w}_1$ and $\bar{w}_2$ here. At the same time, we can notice that the first transmission term $\bar{w}_1$ does not take into account the distant object since its value is fixed at 1. The second transmission term $\bar{w}_2$ may take into account the distant object. In fact, it represents the complementary of $\bar{v}$ in the interval $[0, 1]$.

From this relationship, it is worth mentioning that the minimum envelope $E^{\min}$ is compatible with the DCP since this quantity can be assimilated to the local reference darkness points in each chromatic channel.[13]

Model Development
Model Validation

If we approximate p_{STRESS} in Eq. (8) by $E^{\min}$, then p_{STRESS} is also solving the same model. Since we know that

$p_{\text{STRESS}} \in [0, 1]$, by normalizing its final expression in Eq. (9), we come back again on the initial definition of p_{STRESS} in Eq. (4).

This validation should also take into account measurement from real world to check out how close our model is to the haze model for certain scenarios. For the purpose of simplicity, in this article, we are not going to measure the accuracy between the model behind STRESS and the haze physical model. In fact, from Observation 1 and what we develop below, one can say that the relationship in Eq. (8) has nothing to do with the haze model, since $t_1 = 1$ and $t_2 \in [0, 1]$. Therefore, it is good to underline in this case the fact that the STRESS model is compatible with the haze physical model, but not equivalent to it. From the observation above, it is still hard to say what has influence on the dehazing process: is it the minimum envelope $E^{\min}$ or the relation that we found between the two models? or perhaps both? That is the main reason why we could not say that STRESS is part of the second group: the accuracy of the model needs to be computed before.

Remark 1. In the following, a given variable v will be said low, when there exists $\varepsilon_0 \in [0, 1/2]$ such that $v < \varepsilon_0$. A given variable v will be said high, if there exists $\varepsilon_1 \in [(1/2), 1]$ such that $v > \varepsilon_1$. Also, we will implicitly or explicitly admit the validity of the DCP for near objects and far objects.

Observation 2. *If $p_0 \in [0, (1/2)]$ then p_{STRESS} solves the physical model defined in Observation 1.*

From Ref. 13, we know that $p_0 = E^{\max}$ at the global maximum and $p_0 = E^{\min}$ at the global minimum. So $E^{\max} \in [0, 1]$ and $E^{\min} \in [0, 1]$ since p_0 is normalized in $[0, 1]$. If p_0 is low then p_{STRESS} will behave as $E^{\min}$ since p_{STRESS} is a stretching of p_0 between $E^{\min}$ and $E^{\max}$.

Another parameter which plays a great role in the removing of the fog especially for near objects in this section is the radius parameter R fixed such that $R = \max(image_{\text{width}}, image_{\text{height}}) = \max(w, h)$. This kind of sampling with $R = \max(w, h)$ can be compared to the randomized global sampling method described in Ref. 43 in some way.

Let us see now the impact that this parameter has on the dehazing task. We know from Ref. 13 that the parameter $\bar{v}$ represents the average of v_i as you can see on the third line of Eq. (4).
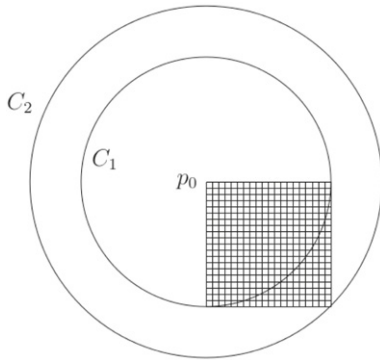
Figure 3. C_1 and C_2 are two circles respectively with $R = max(w, h)$ and $R = \sqrt{w^2 + h^2}$ centered at p_0, the left top pixel.

Observation 3. *Setting the radius parameter R in the STRESS framework for the dehazing task, such that $R = \max(w, h)$ allows to remove fog from near objects at least.*

Thanks to Observation 1, we just need to show here that the transmission $\bar{w}_2$ is high. Since $R = \max(w, h)$, almost all the pixel except p_0 are candidate for the sampling step.

The case where roughly all $v_i = (1/2)$ is not very interesting, because we know that means objects in the middle of our image will be dehazed according to what we said previously and also the radius R for that particular case has no direct effect on $\bar{w}_2$. Now we turn to the other case. Since we know $R = \max(w, h)$, we can say that $s_i^{\max}$ and $s_i^{\min}$ represent well enough the max sample and the min sample, which means that $r_i = s_i^{\max} - s_i^{\min}$ should be high (it is not always the case, but often the case). Since we know also that $v_i = (p_0 - s_i^{\min})/r_i$, then v_i should be less than $1/2$ in that case if p_0 is a near pixel. $\bar{w}_2$ being the complementary of v_i in the interval $[0, 1]$, it follows that $\bar{w}_2$ should be high. Also, $\bar{w}_2$ concords with the transmission and we know that the transmission is inversely proportional to the depth map. The first transmission $\bar{w}_1 = 1$ takes already into consideration near objects as we said previously. From this point of view, we can see that with this configuration near objects are well taken into account by the STRESS framework for the dehazing task. (We can also use Observation 2 to show the idea behind the observation: the pixel intensity of near object are roughly very low. The DCP is also another argument.)

Observation 4. *The optimal setting of R, which allows to take into account near objects is such that $R = \sqrt{image_{\text{width}}^2 + image_{\text{height}}^2} = \sqrt{w^2 + h^2}$.*

Let us consider the following grid (Figure 3) as possible shape (rectangle or square in any case) of our image. Let p_0 be the left top pixel, C_1 represent a circle of radius, $R_1 = \max(w, h)$, and C_2 a circle of radius, $R_2 = \sqrt{w^2 + h^2}$. With the configuration $R = R_2$, all the pixels of the image except p_0 (the pixel in processing) are candidates for the sampling step in STRESS algorithm. Taking $R > R_2$ will not increase the number of candidate samples and also taking $R < R_2$ will not necessarily consider all the pixels except p_0,
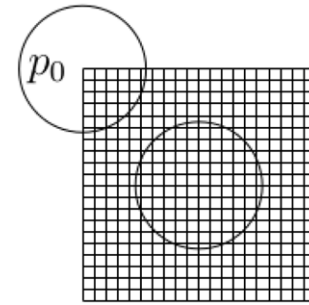

Figure 4. The two circles have a radius r chosen such that $R/10 \leq R = r \leq R/2$ where $R = \sqrt{w^2 + h^2}$ or $R = \max(w, h)$.

since R_2 represents the diagonal of the rectangle image or of the square image.

So, now let us assume that $R = R_2$. It is also obvious that the more pixel we consider for the sampling, more the difference $r_i = s_i^{\max} - s_i^{\min}$ will be large. And that means, we are making an accurate approximation of the global airlight. And since we are considering near objects, p_0 and $v_i = (p_0 - s_i^{\min})/r_i$ will be less than $1/2$. It follows that $\bar{w}_2$ should be high since $\bar{w}_2$ is the complementary of $\bar{v}$ on $[0, 1]$, and the near object well dehazed.

From Observation 4, increasing the radius more than $R = \sqrt{w^2 + h^2}$ will not improve what we already get for near or far objects, so now let us consider how to reduce the radius.

For nonhomogeneous haze, we notice that non-sky far objects are not accurately taken into consideration by the STRESS framework for the configuration where $R = \sqrt{w^2 + h^2}$ or $R = \max(w, h)$.

At first sight, we can guess that by taking a small radius, it is possible to approximate the removing of fog on distant objects accurately. One hypothesis here is that the haze is not dense and we will make an experiment on a heterogeneous one to see whether or not this setting could influence the distant objects.

Empirically we also observe that for non-sky distant objects, the pixel is also high with some variations due to the Dark Channel Prior. When there is no sky it is also quite difficult to make a difference between a non-sky distant object and a sky region for the pixel situated on the top of the image. Later on, we will come back to this particular observation. Let r be the radius such that $(1/10) \max(w, h) \leq R = r \leq (1/2) \max(w, h)$.

Observation 5. *Reducing the radius $R = r$ such that $(1/10) \max(w, h) \leq R = r \leq (1/2) \max(w, h)$ will allow to remove fog from distant objects in nondense heterogeneous haze.*

Let us consider Figure 4 for the idea behind this observation.

If we take the radius r small instead of taking $R = \max(w, h)$, we can see that the distant object of the scene will be well processed. In fact, the difference $r_i = s_i^{\max} - s_i^{\min}$ is not going to be very large and will roughly be less than $1/2$ since we are considering a small spray and far
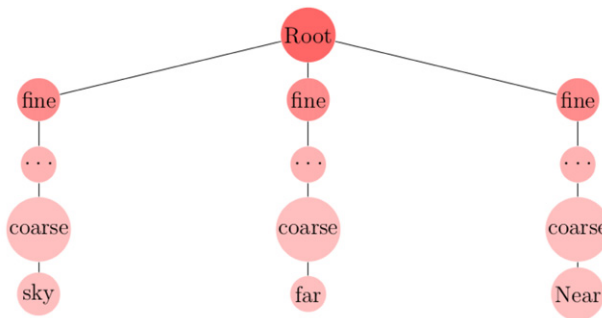
J. Imaging Sci. Technol.
IS&T International Symposium on Electronic Imaging 2016
Color Imaging XXI: Displaying, Processing, Hardcopy, and Applications

010409-5

Jan.-Feb. 2016

COLOR-353.5

Figure 5. General overview of how we model the outdoor hazy image. The root represents the hazy image. We begin at a given leaf and back up to the root. The nodes between a leaf and the root represent an attribute(s) which will allow to refine and determine the real nature of the leaf namely: the sky (or region with the same behavior like snow region), far objects, and near objects. On the last node before the root, we apply a given scale according to the nature of the leaf. An implementation of this tree is showed in Figure 6; coarse and fine stand for coarse scale and fine scale, respectively.

Figure 6. An implementation of Figure 5. We begin by checking the presence or the absence of the sky region, followed by far or near objects. On the right branch, we also check at the node No edge the width and the height of the region.

Remark 2. Every color channel in haze-free image has pixel with high intensity and close to 255, if we consider an image with 8 bit per channel for sky region.

objects. (A far object has a pixel intensity often high and by considering the dark channel for these regions, the difference for neighborhood pixel is not huge.) Also, locally the airlight will be well approximated. The nondensity of haze will allow us to satisfy not only the presence of a background but also the validity of the Dark Channel Prior in some way—The DCP is not directly applied to the output image here but we can easily see that the DCP prior is not anymore valid when the haze is dense. The saturation that we get with dense haze, by using Ref. 18 is already an empirical validation. The other point is that the saturation effect tend to be stronger with a small patch (small spray in our case for sky region).

Since r_i is not large, at least the term $1/r_i$ in the product $(p_0 - s_i^{\min}) * 1/r_i$, will be high and making v_i a bit high. If also $p_0 - s_i^{\min}$ is large then v_i is also high. It follows that $\bar{w}_2$ is low and the haze on distant object well removed. (We can also used Observation 2: since the radius is reduced, all p_0 closed to $E^{\min}$ are good candidates for the dehazing process.)

Empirically, we noticed also that near objects are not really taken into account by small radius, but far objects have a good processing for this configuration. Typically, for near objects, we can easily see that the configuration in which we reduced the radius such that $R \leq (1/2) \max(w, h)$ is not going to improve the visibility of these objects in agreement with what we show in Observations 3 and 4. Depending on how the radius is set, we will work either on globality or locality of the contrast enhancement. Now the idea is to combine different radii in such a way that allows to dehaze far and near objects. Subsequently, we will show how this combination can be done theoretically.

We can also notice that the sky will use a prior derived from Ref. 17. The reason is that the General Dark Channel Prior (GDCP)—see Ref. 57 for more details—could not be valid in the sky, even for blue-sky, we observed that the DCP can be valid. By taking a kind of contrapositive of the DCP, we will have the following statement.
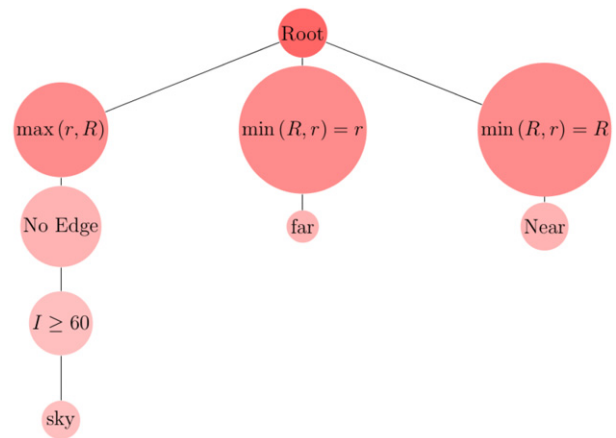
PROPOSED APPROACH

The key idea behind our approach here is inspired from Ref. 44, where it is said concerning HMM that, many complex images, scenes, and phenomena can be modeled as combinations of simple pieces. The other articles which also justify our method are the work of Refs. 45 and 46 for instance, where authors show that it is possible to estimate a random field with a multiscale approach. Even their approaches are different from what we are presenting here, there is some significant similitude. Our work can be compared to the works of Refs. 29, 30 as well. Our work uses other ideas from the literature of course. The image will be modeled as a graph, where each node will represent a given state or attribute.

From what we develop above, we can see that STRESS is solving already the homogeneous (i.e. uniform or stationary) haze case (dense or not). The homogeneous case can be viewed as a single Markov field since we assume there is a single uniform layer that we have to find out. Now, about the heterogeneous case. For the heterogeneous haze, we will also have two cases: one is dense and the other nondense. Here we will focus mainly on developing a model for nondense haze. In fact for the dense case, it is not possible to get more visibility with far objects, simply because the data is not present and for that particular heterogeneous case, the result given by the single scale STRESS is already, one of a pleasing one. Also for that particular case, the dense part will be considered as a sky region and we will process it in the same way that we process the sky. This point will be trivial afterward. Depending on how dense the haze is, we might need to increase the number of samples of STRESS framework parameter, in order to remove noise. The other question is how to guess the number of samples necessary

J. Imaging Sci. Technol.
IS&T International Symposium on Electronic Imaging 2016
Color Imaging XXI: Displaying, Processing, Hardcopy, and Applications

010409-6

Jan.-Feb. 2016

COLOR-353.6

to remove the noise of a given dense haze. The answer to this question will depend on the way we choose to implement our case. In our case, we will consider just a few samples (less than 6).

We can now imagine a model where we can see the heterogeneous nondense haze as a superposition of homogeneous haze layer with different density (without being abrupt). It is worth noticing that both the visible pattern and the hidden pattern actually represent two different layers; the goal being to remove these hazy layers to get the dehazed hidden layers. The challenge will then be to guess which radius value corresponds well to the removing of a haze for a given pixel. We can, for instance, define a cost function which can allow us to choose the best approximation among a finite set of possible approximations. Let us assume that the coarsest scale is given by $R = \max(w, h)$ or $R = \sqrt{w^2 + h^2}$ and the finest one by $R = (1/10)\max(w, h)$ or $R = (1/10)\sqrt{w^2 + h^2}$. Let $p_{\hat{0}, R}$ be the approximation of p_0 given by R and $p_{\hat{0}, r}$ be the approximation of p_0 given by r, so we can write:

$$p_{\hat{0}, R} = P_{\text{STRESS}, R} \bar{w_1}_R + (1 - \bar{w_2}_R)\bar{r}_R \qquad (10)$$
$$\cdots = \cdots$$
$$p_{\hat{0}, r} = P_{\text{STRESS}, r} \bar{w_1}_r + (1 - \bar{w_2}_r)\bar{r}_r. \qquad (11)$$

From the continuity criterion that a well-posed problem should satisfy, the optimization problem match with the following relationship:

$$|J - P_{\text{STRESS}}| < \sigma \Rightarrow |p_0 - p_{\hat{0}}| < \varepsilon. \qquad (12)$$

$p_{\hat{0}, s}$ represents a given scale s of the STRESS framework and $p_{\hat{0}}$ corresponds to the approximation of p_0 at the same scale s. Since we are dealing with a multiscale approach, the parameter J we are looking for can be obtained as follows:

$$J = \text{argmax}(P_{\text{STRESS}, R}, \ldots, P_{\text{STRESS}, r}). \qquad (13)$$

The problem we want to solve here is a nonstationary problem. The idea is to carry out some piecewise cut of the image in a such a way that each piece could represent a stationary problem. In order word, we are going to solve the problem by combining STRESS with Hidden Markov Model (HMM) and solve the dehazing issue. Formally speaking, the idea consists of using the Bayes rule in order to check the probability of our hypothesis according to the observed samples and by stating the following equation:

$$p(H \mid O) = \frac{p(O \mid H) \cdot p(H)}{p(O)}, \qquad (14)$$

where H stands for the hypothesis (the final dehazed layer) and O for the observation (the hazy input image). $p(H \mid O)$ is called the posterior probability or the probability of H given O, that is the probability of having H after observing O. $p(O \mid H)$ is the likelihood and represents the probability of observing O given H. $p(H)$ is the prior probability or simply the prior and represents the probability of the hypothesis H before O is observed. $p(O)$ is the marginal likelihood. This

factor is the same for all possible hypotheses and can be considered necessary only for normalization purposes. So Eq. (14) can be also written:

$$p(H \mid O) = p(O \mid H) \cdot p(H). \qquad (15)$$

Let us assume l being a set of hidden haze-free layers, l_i is a given haze-free layer (corresponding to a visible layer) in the image and let us say here that the number of layers in the foggy image is $|l|$ such that $1 \leq i \leq N$ and $N \geq 1$. For the problem we are discussing here, if we call I the observed foggy image then we can express the posterior probability as the following:

$$p(l_1, \ldots, l_N \mid I) \propto p(I \mid l_1,) \ldots p(I \mid l_N) \cdot p([l_1 \cdots l_N]) \quad (16)$$

or we can also write the following equivalent form:

$$p(\underline{l} \mid I) \propto \prod_{1 \leq i \leq |l|} p(I \mid l_i)p(\underline{l}), \qquad (17)$$

where $\underline{l} = [l_1, \ldots, l_N]$ is a vector. In the literature to solve Eq. (17), since we have a multiplicative factor, it is better to use the logarithm function. In that case, the equation can be written down as follows:

$$-\log(p(l_1, \ldots, l_N \mid I)) = -\log\left(\prod_{1 \leq i \leq N} p(I \mid l_i)p(\underline{l})\right). \quad (18)$$

If we adopt the same notation as in Ref. 47 by separating respectively in the likelihood term and the prior term, we can then write the above relation as the following:

$$-\log(p(l \mid I)) = \Lambda(l) + \Pi(l). \qquad (19)$$

The goal of this approach is to choose the posteriori, which represents well what we are looking for (get a good dehazed version of the hazy image). That is:

$$\hat{l} \propto \text{argmax } p(l_1, \ldots, l_N \mid I) \qquad (20)$$
$$\propto \text{argmax } p_{\text{multi\_scale\_STRESS}}. \qquad (21)$$

$\hat{l}$ is called the maximum of the posterior probability density function a.k.a the Maximum A Posteriori (MAP) and stands for the best nonfoggy layer we are looking for. As for the way we are designing our model, it is possible to see $\hat{l}$ as one of the best layer corresponding to a given visible layer (i.e. $\hat{l}_i$ more specifically) or as the best final layer of the entire image resulting from the combination of each best layer. So here we will take the last description as how we will consider the formula Eq. (20). To solve Eq. (20), since we have an ill-posed problem, in the literature, we have often got to use some optimization algorithms like graph-cut or a Laplacian regularization. In our case, the good news is that with STRESS we can already find a good approximation of the layers we are looking for as we show above in the previous development: For near objects (near objects, sky region, and regions which have the same behavior with the sky like large

snow area. We will notice this in the following lines.), the radius is R and for far objects the radius is r.

So now the problem can be summarized as the following: For a given pixel in the input which single scale STRESS represents the best layer for the dehazing task? For simplicity purpose, we will solve the problem using a two scale. The choice of the two scale can be justified by what we observed empirically and the cost of the final solution. And there is still a link between the STRESS model and the two-scale STRESS. In fact, one can see that the two-scale STRESS can be viewed as two envelopes, one representing upper-bound envelope $E_{\text{two-scale-STRESS}}^{\max}$ and the other, the lower-bound envelope $E_{\text{two-scale-STRESS}}^{\min}$. Since the output pixel of the two-scale STRESS is a potential solution of our problem, how are we going to remember which one is the best? The formulation of the DCP will help us to do it in some way. In this work we do not use the DCP directly but our procedure seems to be near to that idea. It is also good to remember that STRESS does not consider patches in the rectangular way but in the circular fashion. So the theoretical transition probability corresponding to the coarsest prior to the finest one—the coarse-to-fine transition probabilities [48]—is as the following:

$$p(l_{k+1} \mid l_k \ldots l_0) = p(l_{k+1} \mid l_k), \tag{22}$$

where $(k + 1) \in \{0, 1\}$ and $k \in \{0, 1\}$ (equivalently, we can write $(k + 1) \equiv 0 \bmod 2$ or $(k + 1) \equiv 1 \bmod 2$ and $k \equiv 0 \bmod 2$ or $k \equiv 1 \bmod 2$) since we are considering just two scale. So from the definition of the prior in Eq. (22) the J parameter we are hunting can be assessed when the following formula holds for near and far objects:

$$\text{argmax}(|p_0 - p_{0,\hat{R}}|, |p_0 - p_{0,\hat{r}}|) \sim \min(P_{\text{STRESS},R}, P_{\text{STRESS},r}). \tag{23}$$

Our idea for applying this transition is of course by choosing the minimum pixel value (the dark channel) for each channel between the results given by the two scale. One drawback by choosing the dark channel and just two scale (instead of multiscale) can be the smoothness issue of the final output and also the scales can be mixed. Theoretically, for far objects, we know that the output pixel intensity with the radius r should be lower than the output pixel intensity value with the radius R and we have the inverse scenario with near objects. However, even if in practice, the previous assertions are true for a majority of cases, it may happen that they are false for some pixels. And for those cases, by choosing the minimum pixel intensity value, the scales output are going to be mixed since we have 3 channels (total order versus partial order problem[49]). On the other hand, the advantage of this modeling is simplicity.

There are many ways in the literature to detect the sky as the one in Ref. 55; other segmentation approaches such as graph-cut, Gibbs model, annealing, Local Binary Pattern (LBP) can be used too. In our case, due to simplicity purposes, we choose an edge detection approach that we combine with the HMM idea.

The main idea behind the edge detection strategy (for this first implementation) is that we notice in most cases in hazy images and their corresponding haze-free images that the sky a priori does not contain any edge since we do not have cloud often in hazy images. And even if it is possible to find clouds on a hazy image, they are very rare and their proportions are not significant.

The second reason is that, the sky is on the top region in the image, which means that the first edge which can be found will belong to far objects in the case of a nonhomogeneous haze and to near objects in the case of a homogeneous haze.

The third reason why we choose the edge detection at this stage can be assigned to the fact that in the image in which we do not have the sky, we do have a high intensity value for the pixel which is in the top lines of the image. In that case, if we just consider a labeling with high pixel intensity value for segmentation, we can easily make a false detection—false positives—of the sky region. We are not saying that our strategy is unquestionable but we will show later in the experiment part that this approach is robust at least for all images that we tested from state-of-the-art dehazing articles and from our database.

Another strong reason is the fact that we want to check quickly the hypothesis that we could make one the sky region and still have an output which looks natural.

The decision of finding a potential sky region is based on the fact that we do not have any edge on the top of the image, the pixel intensity is also greater than 60. Furthermore, the area which has these two attributes (no edge and *intensity* >60) should represent at least 5% of the total height of the image and 50% of the total width. We will call this approach the trip concept.[57]

EXPERIMENT AND RESULTS

The experiment setup is almost the same as in Ref. 54, except the fact that we design here our own algorithm for dehazing based on the STRESS and we also consider here a psychophysical experiment. In our experiment, we consider three types of images. Images taken in Gjøvik, images from NRK, and images from state-of-the-art algorithms. Gjøvik pictures and the ones from NRK are initially very large and make the computation time really high. To avoid this, we reduce the original size to $1128 * 751$ for Gjøvik pictures and $1128 * 635$ for NRK pictures. All the codes that we have were run on the following machine: Ubuntu 14.04 LTS, with 8GIB of memory, Intel Xeon (R) CPU E31270 and 3.45 GHZ $* 8$. The number of images processed is more than 200.

For Gjøvik pictures, the original images have size of $4290 * 2856$ and format CR2 from a camera model Canon 450D. Then we use dcraw software to convert the initial file into BMP files. From the obtained files, we use next ImageMagick to resize all the image to $1128 * 751$.

For NRK pictures, the original frames have size of $1920 * 1080$, we do exactly the same procedure as previously except the fact that we use VLC software to extract images from videos. The retrieved files have finally a size of

J. Imaging Sci. Technol.   010409-8   *Jan.-Feb. 2016*
IS&T International Symposium on Electronic Imaging 2016
Color Imaging XXI: Displaying, Processing, Hardcopy, and Applications   COLOR-353.8

Table I. Metric-based experiment on state-of-the-art images. In this table, as you can see our method gives quite good results in terms of rate of new edges e, except for the last column, where it has been out performed by STRESS.

e	Snow	Building	Canon	Lviv
DC	2.32	0.03	3.02	0.21
Fattal 14	1.79	−0.02	3.44	0.25
STRESS	2.77	0.05	2.83	0.40
Ours	4.22	0.07	3.44	0.34

Table II. Metric-based experiment on state-of-the-art images. Our method yields the best visibility for images Snow and Canon. Since we have four images for this series, we can say that our method is the best with this metric. In fact, for Lviv we have the second best result and for Building, we are in the third place.

$\bar{r}$	Snow	Building	Canon	Lviv
DC	2.67	2.31	6.43	3.27
Fattal 14	3.92	3.13	6.29	1.52
STRESS	4.60	1.92	4.68	1.87
Ours	5.10	2.24	8.32	2.13

Table III. Metric-based experiment on state-of-the-art images. According to this metric relative to the saturation rate, the proportion of saturated pixels in our method, after dehazing, is always less than 2.5%.

σ	Snow	Building	Canon	Lviv
DC	0.04	2.60	1.23	1.73
Fattal 14	1.19	12.8	21.87	0.02
STRESS	0.39	1.52	0.31	1.92
Ours	0.57	1.82	0.50	2.22

$1128 * 635$. In the following, we call our database, Gjøvik pictures or NRK pictures.

In Ref. 53, the authors said that the variables e and $\bar{r}$ should be high. σ should be low. The variable e represents the rate of new visible edges between the original hazy image and its restored (dehazed) version. This parameter allows us to evaluate the proportion of edges which are in the restored image but not in the original one. $\bar{r}$ represents the geometric mean of the ratio of Visibility Level (VL) and according to Ref. 53, $\bar{r}$ reflects the quality of the contrast restoration. The last parameter σ illustrates the normalized rate of saturated pixels in the restored image. As we can see in Figure 8, column (e), the last metric σ does not really take into account the saturation effect, the way it is supposed to do.

In the case of the psychophysical experiment (Tables IV and VIII), we use a web-based tool for psychometric image evaluation tool named QuickEval.[56] It is good noting that the experiment is made in an uncontrolled environment. According to Ref. 57, research have shown small differences between controlled (in a laboratory) and uncontrolled

Table IV. Psychophysical experiment on state-of-the-art images. The experiment shows that DC and STRESS have more visibility than others. The good news for us, on this series, is the fact that the variance is not huge between the best and the worst. We can say from that perspective, there is no significant difference between the output produced by these algorithms.

Z-score	Snow	Building	Canon	Lviv
DC	0.041	0.36	0.032	0.34
Fattal 14	−0.122	−0.043	−0.035	3.44
STRESS	0.064	0.038	0.027	0.059
Ours	−0.017	−0.039	−0.12	−0.55

Table V. Metric-based experiment on our database. The best result for the e metric along with this series is given by (e). Except for image NRK1, the performance of our approach seems to be close to the best.

e	NRK1	NRK2	Gj1	Gj2	Gj3
(b)	0.76	0.28	0.06	0.27	0.44
(c)	87.87	2.95	0.07	1.41	1.71
(d)	81.51	2.21	0.67	1.15	1.78
(e)	123.36	4.06	2.27	2.50	3.13
(f)	82.27	2.13	1.61	1.16	1.74
(g)	85.27	2.32	0.14	1.31	1.65
(h)	76.05	3.14	0.49	1.49	1.83

Table VI. Metric-based experiment on our database. Taking the r metric with this series allows us to have the best result.

$\bar{r}$	NRK1	NRK2	Gj1	Gj2	Gj3
(b)	1.42	1.45	0.77	1.36	1.24
(c)	3.92	2.34	1.56	$1.96e^{-04}$	2.09
(d)	3.30	1.65	1.59	0.06	2.11
(e)	7.49	5.05	3.50	2.98	2.98
(f)	5.15	1.46	2.16	2.18	1.96
(g)	10.00	2.81	1.36	2.46	2.04
(h)	21.25	5.31	1.86	4.18	3.91

Table VII. Metric-based experiment on our database. Here also, for our approach the proportion odf saturated pixels, according to the σ metric is less than 2.5%.

σ	NRK1	NRK2	Gj1	Gj2	Gj3
(b)	0.00	0.01	$3.93e^{-05}$	0.00	0.00
(c)	0.04	0.04	0.00	2.26	0.00
(d)	1.34	1.39	0.08	2.36	0.03
(e)	1.66	1.72	0.00	0.00	0.00
(f)	0.99	1.62	0.18	0.01	0.01
(g)	1.50	1.53	0.41	0.27	0.29
(h)	2.12	1.86	1.08	0.91	1.04

J. Imaging Sci. Technol.   010409-9   *Jan.-Feb. 2016*
IS&T International Symposium on Electronic Imaging 2016
Color Imaging XXI: Displaying, Processing, Hardcopy, and Applications   COLOR-353.9
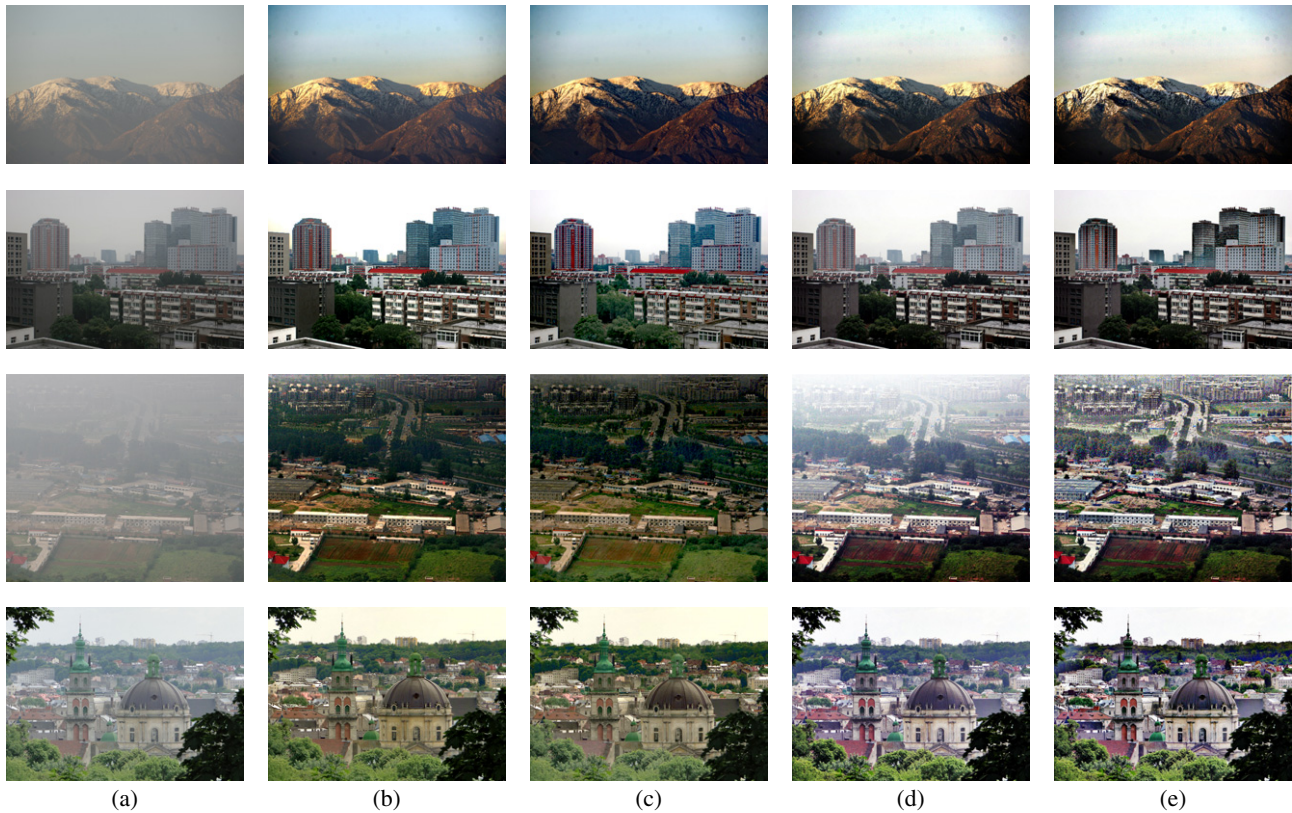
|(a)|(b)|(c)|(d)|(e)|

Figure 7. From top to bottom on each line, the original image represents respectively Snow, Building, Canon, and Lviv. From left to right on each line, we have the original image (a), DC or DCP (b), Fattal 14 (c), STRESS with $n_i = 150$ and $n_s = 5$ (d), our method using STRESS with the same parameters (e). For the second line series, considering our method, we can see there is a smoothness issue on the immediate boundaries between the sky region and the buildings. This issue can be solved by processing these immediate boundaries in different ways.
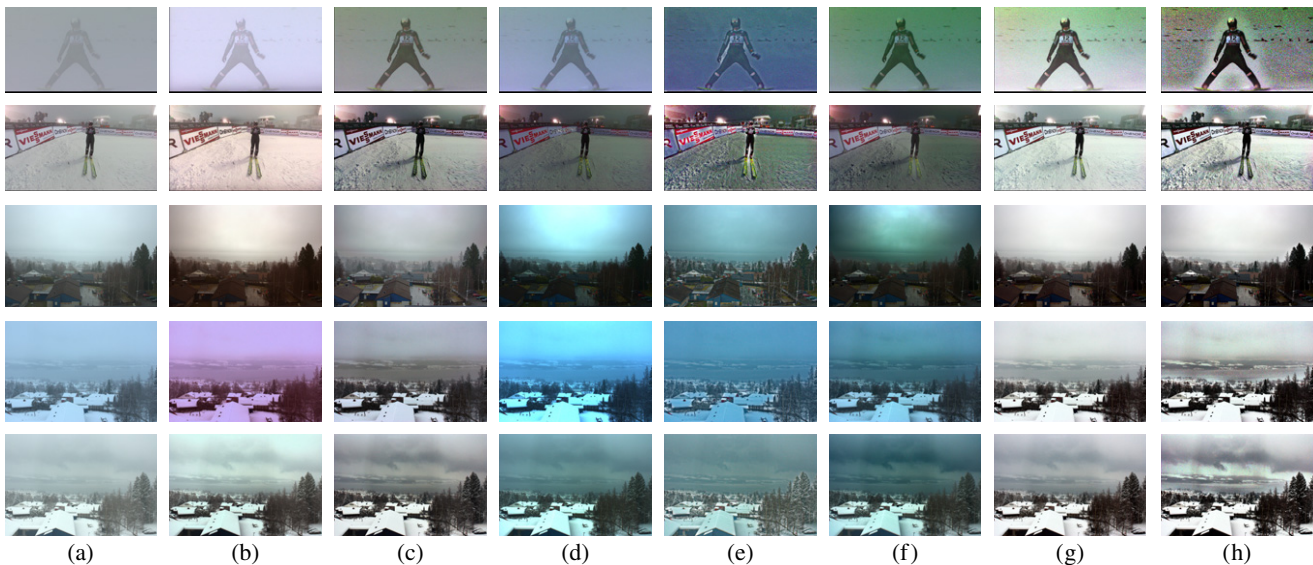

|(a)|(b)|(c)|(d)|(e)|(f)|(g)|(h)|

Figure 8. From top to bottom, on each line, the original corresponds respectively to NRK 1, NRK 2, Gjøvik 1, Gjøvik 2, Gjøvik 3. For images taken in Gjøvik, we can see the Lake Mjøsa—in winter 2014/2015. From left to right, we have original hazy image (a), McCann (b), ACE (c), Gibson (d), Tarel (e), DCP (f), STRESS with $n_i = 150$ and $n_s = 5$ (g), and finally our method with the same parameters (h).

experiments (on the internet). In our experiment, 15 people have done the experiment in the lab and 4 people on the web. We do not notice a particular difference between these two

experiments, except the fact that the experiment takes less time for people who have done it in the lab. That makes sense, since participants who did the experiment in the lab, have a

Table VIII. Psychophysical experiment on our database. For this evaluation, as you can see, our method gives always a positive Z-score for all three images which have been evaluated. Here again, the goal is to rank images according to their visibility level.

Z-score	NRK2	Gj1	Gj2
(b)	0.58	0.45	−0.21
(c)	−0.21	0.37	0.53
(d)	−0.91	−0.06	0.27
(e)	−0.38	−0.42	−0.86
(f)	−0.34	−0.51	0.65
(g)	0.30	0.07	−0.71
(h)	0.56	0.32	0.10

direct explanation of the instructions to follow from us. For the experiment done in the lab, these 3 conditions have been fulfilled. The presentation of stimuli is done via a monitor. The area immediately surrounding the displayed image and its borders has a neutral dark gray color.

In Tables I and V, where we compute the rate of visible edges between the original image and the restored one, the results given by STRESS and our method based on STRESS are often quite good compared to others. The experiment shows also that Ref. 24 seems to be well adapted to this metric. When considering NRK1 for instance, the only image where we get almost the worst metric, it seems that the metric concords as well with what we get visually. As you can see, there is a halo around the athlete in our output. On the worst evaluation given by Retinex, the output effectively does not look dehazed; Paradoxically, the output given by Ref. 24 has halo as well, but their evaluation is the best for this series.

For the second metric that we use (Tables II and VI), which reflects the quality of the contrast restoration, it seems that STRESS and our method outperform the other as you can see with NRK1. Since our main goal is to get more visibility in bad weather, we can say that we are close to our objective.

For the last metric (Tables III and VII), which should reflect the proportion of saturated pixels in the output image, it seems that, we have again contradictory results, since our output images look less saturated than the output of Ref. 24 but they have got better evaluation than we have.

Considering state-of-the-art images (32 images in total), this experiment shows that generally the metric-based evaluation gives good results for 2/3 of parameters and psychometric-based one gives an acceptable result considering state-of-the-art images. Taking into account images from our database, the experiment shows that both the metric-based and psychometric-based evaluation give good results for our method.

It is also worth noticing that the work that we present here has some limitation, for example, the pixel state estimation with regard to the sky region. Moreover, we do not make any assumption on the input image, except that it is hazy. At the same time, an image can look hazy but the noise which makes it hazy is not related to the haze phenomenon.

So if the image which we are going to process look hazy, then how accurate is the model (the haze physical model or STRESS model) for enhancing the input image? And what if the noise does not come from haze or fog but looks like haze or fog? To answer the latter, in ongoing work, we make a series of tests, where we place in front of a camera, and close to it, a plexiglass, that we scratch with different intensities to simulate the degree of haziness. The first conclusion is that, we are losing a significant amount of data coming from the scene in this scenario, so that our method is not able to recover these lost data. We can also say that even STRESS can dehaze a natural hazy image, it could not be used as a decoder for any kind of hazy image. There is still a point which needs more discussion as the assumption made on the sky region or the model that we use for dehazing task: how much the output given by STRESS model is close to the ground truth? Here, theories developed by McCann and Rizzi in Ref. 4 could provide some answer to this question. One of these theories is that when human vision looks at high-dynamic range displays, it processes scenes using spatial comparisons.[56]

CONCLUSION

We develop in this article, a new dehazing algorithm based on the STRESS model, which is similar to the classical one developed in Eq. (1). We also validate our new algorithm theoretically and empirically. From this, can we say that the STRESS framework is a hybrid algorithm? To answer this question, in a future work we are planning to measure the accuracy of the STRESS model. It is also good to notice that the haze model and the STRESS model are not equivalent; and how the models are close to each other will be addressed in a future work as well.

In the first part of our work, we show that the STRESS framework can be seen as a good heuristics for the dehazing task as far as homogeneous (or dense) haze is taken into consideration.[54] Furthermore, we demonstrate that we can find some resemblance between the classical haze model parameters in Eq. (2) and the model derived from STRESS. As a consequence, the estimation problem of the dehazing task falls into the state estimation of a given pixel.

In the second part, we then model the outdoor hazy image in three regions where each represents a stationary problem in the sense of Hidden Markov Model (HMM) approach, namely: near objects, far objects, and sky region (and region similar to the sky region as snow region). These three regions can be seen as the state variables of our model sharing a common attribute: the radius parameter of the STRESS framework.

The radius parameter is crucial for the defogging problem and helps us to have a good assessment of the other parameters in the haze model that we develop. Therefore, the airlight and the pseudo-transmission in our model are estimated in two ways. The first one consists of assessing these two parameters globally in the case of near objects and sky region. The second one falls in with the estimation of the parameters locally in the case of far objects.

J. Imaging Sci. Technol.
IS&T International Symposium on Electronic Imaging 2016
Color Imaging XXI: Displaying, Processing, Hardcopy, and Applications

010409-11

Jan.-Feb. 2016

COLOR-353.11

To achieve the globality and the locality principles, we use the two-scale STRESS by defining two different radii. Furthermore, these two radii are chosen in the way that we can have an aerial perspective in the image output. Even if we have some cases of failure, we show empirically that it is possible to overcome some color fidelity case by having a formal labeling of the hazy image, since dehazing does not preserve the color fidelity.[55] We show that our method can be better than some of the state-of-the-art approaches in terms of visibility and using the metrics defined in Ref. [53].

In future work, we are planning to test our algorithms on more images including fog simulated in the context of indoor applications and also on video outdoor applications.

REFERENCES

[1] A. Aponso and N. Krishnarajah, "Review on state of art image enhancement and restoration methods for a vision based driver assistance system, with de-weathering," Soft Comput. Pattern Recognit. 135–140 (2011).

[2] S. Narasimhan and S. Nayar, "Vision and the atmosphere," Int. J. Comput. Vis. **48**, 233–254 (2001).

[3] R. Ajaj, N. Delprat, and C. Jacquemin., "The fog as a simulation object: from sensorial perception to imaginary aspects," Journée d'étude STMA, BétonSalon, Paris (2009).

[4] J. J. McCann and A. Rizzi, The Art and Science of HDR Imaging (J. Wiley, Chichester, 2012).

[5] K. Gibson, S. Belongie, and T. Q. Nguyen, "Example based depth from fog, Image Processing (ICIP)," 20th IEEE Intl. Conf. (IEEE, Piscataway, NJ, 2013), pp. 728–732.

[6] S. Narasimhan and S. Nayar, "Contrast restoration of weather degraded image," IEEE Trans. Pattern Anal. Mach. Intell. **25**, 713–724 (2003).

[7] Wikipedia, Aerosol, https://en.wikipedia.org/wiki/Aerosol (as of Oct. 25, 2015).

[8] E. J. McCartney, Optics of the Atmosphere (John Wiley, New York).

[9] Wikipedia, Mie scattering, https://en.wikipedia.org/wiki/Mie_scattering (as of Jul. 13, 2015).

[10] M. Mishchenko, L. Travis, and A. Lacis, "Optical models for color reproduction," NASA Goddard Institute for Space Studies (2005).

[11] L. Simonot, M. Hébert, R. Hersch, and H. Garay, "Ray scattering model for spherical transparent particles," J. Opt. Soc. Am. A **25**, 1521–1534 (2008).

[12] A. Rizzi, C. Gatta, and D. Marini, "A new algorithm for unsupervised global and local color correction," Pattern Recognit. Lett. **24**, 1663–1677 (2003).

[13] Ø. Kolås, I. Farup, and A. Rizzi, "Spatio-temporal retinex-inspired envelope with stochastic sampling: a framework for spatial color algorithms," J. Imaging Sci. Technol. **55**, 0405031 (2011).

[14] B. Xie, F. Guo, and Z. Cai, "Improved single image dehazing using dark channel prior and multi-scale retinex," Proc. 2010 Intl. Conf. on Intelligent System Design and Engineering Application (2010), pp. 848–851.

[15] J. Kopf, B. Neubert, B. Chen, M. F. Cohen, D. Cohen-Or, O. Deussen, M. Uyttendaele, and D. Lischinski, "Deep photo: Model-based photograph enhancement and viewing," ACM Trans. Graph. (Proc. SIGGRAPH Asia 2008) **27**, 116:1–116:10 (2008).

[16] H. Zhang, Q. Liu, F. Yang, and Y. Wu, "Single image dehazing combining physics model based and non-physics model based methods," J. Comput. Inf. Syst. **9**, 1623–1631 (2013).

[17] W. Wang and L. Xu, "Retinex algorithm on changing scales for haze removal with depth map," Int. J. Hybrid Inf. Technol. **7**, 353–364 (2014).

[18] K. He, J. Sun, and X. Tang, "Single image haze removal using dark channel prior," IEEE Conf. on Computer Vision and Pattern Recognition (CVPR) (IEEE, Piscataway, NJ, 2009), pp. 1956–1963.

[19] H. Tsutsui, S. Yoshikawa, H. Okuhata, and T. Onoye., "Halo artifacts reduction method for variational based realtime retinex image enhancement," Signal & Information Processing Association Annual Summit and Conf. (APSIPA ASC) (Asia-Pacific, Hollywood, CA, 2012).

[20] A. Galdran, J. Vazquez-Corral, D. Pardo, and M. Bertalmío, "A variational framework for single image dehazing," European Conf. on Computer Vision Workshops (2014).

[21] R. Fattal, "Single image dehazing," ACM Trans. Graph. **27**, 72:172:9 (2008).

[22] R. Fattal, "Dehazing using color-lines," ACM Trans. Graph. **34**, 13:113:14 (2014) ISSN 0730-0301.

[23] R. Tan, "Visibility in bad weather from a single image," Proc. IEEE CVPR (IEEE, Piscataway, NJ, 2008).

[24] J.-P. Tarel and N. Hautière, "Fast visibility restoration from a single color or gray level image," Proc. IEEE Intl. Conf. on Computer Vision (ICCV09) (IEEE, Piscataway, NJ, 2009), pp. 2201–2208.

[25] K. Gibson, D. Vo, and T. Q. Nguyen, "An investigation of dehazing effects on image and video coding," IEEE Trans. Image Process. **21**, 662–673 (2012).

[26] K. Gibson and T. Nguyen, "On the effectiveness of the dark channel prior for single image dehazing by approximating with minimum volume ellipsoids," IEEE Intl. Conf. on Acoustics, Speech and Signal Processing (ICASSP) (IEEE, Piscataway, NJ, 2011), pp. 1253–1256.

[27] K. B. Gibson and T. Q. Nguyen, "An analysis of single image defogging methods using a color ellipsoid framework," EURASIP J. Image and Video Processing **2013**, 37 (2013).

[28] K. B. Gibson and T. Q. Nguyen, "Fast single image fog removal using the adaptive wiener filter," IEEE Intl. Conf. on Image Processing (ICIP) (IEEE, Piscataway, NJ, 2013), pp. 714–718.

[29] L. Kratz and K. Nishino, "Factorizing scene albedo and depth from a single foggy image," IEEE 12th Intl. Conf. on Computer Vision (IEEE, Piscataway, NJ, 2009), pp. 1701–1708.

[30] K. Nishino, L. Kratz, and S. Lombardi, "Bayesian defogging," Int. J. Comput. Vis. **98**, 263–278 (2012).

[31] P. Carr and R. Hartley, "Improved single image dehazing using geometry," Digital Image Computing: Techniques and Applications (DICTA 09) (2009), pp. 103–110.

[32] K. Dabov, A. Foi, V. Katkovnik, and K. Egiazarian, "Image denoising by sparse 3d transform domain collaborative filtering," IEEE Trans. Image Process. **16**, 2080 (2007).

[33] Y. Schechner, S. Narasimhan, and S. Nayar, "Instant dehazing of images using polarization," Proc. 2001 IEEE Computer Society Conf. on Computer Vision and Pattern Recognition, CVPR 2001 (IEEE, Piscataway, NJ, 2001), vol. 1, pp. I325–I332.

[34] Y. Zhu, J. Liu, and Y. Hao, "An single image dehazing algorithm using sky detection and segmentation, in Image and Signal Processing," The 7th Intl. Congress on Image and Signal Processing (CISP) (2014), pp. 248–252.

[35] X. Fan, Y. Wang, R. Gao, and Z. Luo, "Haze editing with natural transmission," Vis. Comput. **111**, (2015).

[36] X. Liu and J. Y. Hardeberg, "Fog removal algorithms: a survey and perceptual evaluation," European Workshop on Visual Information Processing (EUVIP) (Paris, France, 2013).

[37] A. T. Islam and I. Farup, "Spatio-temporal colour correction of strongly degraded movies," Proc. SPIE **7866**, 78660Z (2011).

[38] G. Simone and I. Farup, "Spatio-temporal retinex-like envelope with total variation," Proc. IS&T's CGIV2012: 6th European Conf. on Colour in Graphics, Imaging, and Vision (IS&T, Springfield, VA, 2012), pp. 176–181.

[39] D. Shaked and R. Keshet, Robust recursive envelope operators for fast retinex, Technical Report, HP Laboratories Israel, Technion City, Haifa 32000, Israel (2002).

[40] E. Provenzi, M. Fierro, A. Rizzi, L. De Carli, D. Gadia, and D. Marini, "Random spray retinex: A new retinex implementation to investigate the local properties of the model," IEEE Trans. Image Process. **16**, 162–171 (2007).

[41] B. Funt, F. Ciurea, and J. Mccann, "Retinex in Matlab," J. Electron. Imaging 112–121 (2000).

[42] P. Getreuer, "Automatic color enhancement (ACE) and its fast implementation," Image Process. **2**, 266–277 (2012).

[43] K. He, C. Rhemann, C. Rother, X. Tang, and J. Sun, "A global sampling method for alpha matting," IEEE Conf. on Computer Vision and Pattern Recognition (CVPR) (IEEE, Piscataway, NJ, 2011), pp. 2049–2056.

[44] P. Fieguth, "Statistical image processing and multidimensional modeling," Information Science and Statistics (Springer, New York, 2011).

45 K. Chou, A. Willsky, A. Benveniste, and M. Basseville, "Recursive and iterative estimation algorithms for multiresolution stochastic processes," *Proc. 28th IEEE Conf. on Decision and Control* (IEEE, Piscataway, NJ, 1989), vol. 2, pp. 1184–1189.

46 C. Graffigne, F. Heitz, P. Perez, F. J. Preteux, M. Sigelle, and J. B. Zerubia, "Hierarchical Markov random field models applied to image analysis: a review," Proc. SPIE **2568**, (1995).

47 K. M. Hanson, "Introduction to Bayesian image analysis," *Medical Imaging 1993: Image Processing 1898(1)* (SPIE, 1993), pp. 716–731.

48 P. Perez, "Markov random fields and images," CWI Quart. 413–437 (1998).

49 H. Deborah, N. Richard, and J. Y. Hardeberg, "Spectral ordering assessment using spectral median filters," *Mathematical Morphology and Its Applications to Signal and Image Processing*, edited by J. A. Benediktsson, J. Chanussot, L. Najman and H. Talbot, Lecture Notes in Computer Science (Springer, 2015), Vol. 9082, pp. 387–397.

50 A. Gallagher, J. Luo, and W. Hao, "Improved blue sky detection using polynomial model fit," *Intl. Conf. on Image Processing, ICIP 04* (2004), Vol. 4, pp. 2367–2370.

51 K. V. Ngo, J. Storvik Jr., C. A. Dokkeberg, I. Farup, and M. Pedersen, "QuickEval: A web application for psychometric scaling experiments," Proc. SPIE **9396**, 939–624 (2015).

52 I. Sprow, Z. Baranczuk, T. Stamm, and P. Zolliker, "Web-based psychometric evaluation of image quality, Image Quality and System Performance VI," Proc. SPIE **7242**, 72420A (2009).

53 N. Hautière, J.-P. Tarel, D. Aubert, and E. Dumont, "Blind contrast enhancement assessment by gradient ratioing at visible edges," Image Anal. Stereology J. **27**, 8795 (2008) iii, 2, 27, 81.

54 V. Whannou de Dravo and J. Y. Hardeberg, "STRESS for dehazing," *Colour and Visual Computing Symposium (CVCS)* (2015), pp. 1–6.

55 J. El Khoury, J.-B. Thomas, and A. Mansouri, "Does dehazing model preserve color information?," *Tenth Intl. Conf. on Signal-Image Technology and Internet-Based Systems (SITIS)* (Nov. 2014), pp. 606–613.

56 J. J. McCann and A. Rizzi, "Camera and visual veiling glare in HDR images," J. Soc. Information Display **15**, 721–730 (2007).

57 V. Whannou de Dravo, "*Dehazing with STRESS*," Master's thesis (Gjøvik University College, 2015).